Spatial filters for high-peak-power multistage laser amplifiers

A. K. Potemkin, T. V. Barmashova, A. V. Kirsanov, M. A. Martyanov, E. A. Khazanov,* and A. A. Shaykin

Institute of Applied Physics, Russian Academy of Sciences, 46 Uljanov Street, 603950 Nizhny Novgorod, Russia

*Corresponding author: khazanov@appl.sci-nnov.ru

Received 7 November 2006; revised 31 March 2007; accepted 2 April 2007; posted 2 April 2007 (Doc. ID 76877); published 20 June 2007

We describe spatial filters used in a Nd:glass laser with an output pulse energy up to 300 J and a pulse duration of 1 ns. This laser is designed for pumping of a chirped-pulse optical parametric amplifier. We present data required to choose the shape and diameter of a spatial filter lens, taking into account aberrations caused by spherical surfaces. Calculation of the optimal pinhole diameter is presented. Design features of the spatial filters and the procedure of their alignment are discussed in detail. © 2007 Optical Society of America

OCIS codes: 110.6770, 140.3280, 080.3620.

1. Introduction

Solid-state lasers with pulse energies ranging from tens of joules to several kilojoules and pulse durations from tenth fractions to tens of nanoseconds are required for a number of applications, such as inertial confinement fusion [1–5] and intense femtosecond pulse generation either by directly amplifying chirped pulses in Nd:glass amplifiers [6–8] or by using them for pumping of Ti:sapphire amplifiers [9] and optical parametric amplifiers [10–12]. The high-pulse-energy lasers are typically composed of a chain of laser amplifiers with a diameter increasing from input to output. Transport telescopes in these lasers are required to match the beam diameter with the amplifier apertures [5]. In addition, they relay images of successive planes passing through active elements (AEs) of the amplifiers, thereby lowering the beam intensity variations in the AEs [13]. Pinholes in the focal plane of the telescope lenses decrease the angle of view of the amplifiers to prevent parasitic lasing caused by parasitic reflections from various elements, lower the level of amplified spontaneous emission [14], and suppress small-scale self-focusing [15]. Transport telescopes with a pinhole are called spatial filters (SFs) since they filter out high-frequency components of the spatial spectrum. The quality of lenses and telescope alignment governs the laser beam quality, whereas the quality of mechanical elements of the filter (lens mounts, telescope casing mounts, pinhole mounts, and alignment unit) determines the stability and reliability of the laser. For these reasons, spatial filters may be viewed as one of the key elements of intense laser systems.

The theoretical aspects of the above-mentioned functions of SFs have been widely described in the literature ([5,14] and many other publications). The telescope lenses discussed in those papers were considered to be aberration free. In practice, however, lenses are mainly made with spherical surfaces. Such lenses do have aberrations that must be taken into account when designing transport telescopes. Also, little attention has been given to such important issues as choosing an optimal diameter of the pinhole, pinhole alignment procedure, and design features of SFs.

In this paper we describe SFs used in a Nd:glass laser with a pulse energy up to 300 J and a pulse duration of 1 ns. This laser is designed for pumping of a chirped-pulse parametric amplifier [11]. In Section 2, we present data required to choose a SF lens, taking into account aberrations caused by spherical surfaces. Section 3 describes the procedure of choosing

0003-6935/07/204423-08$15.00/0

the pinhole size. Design features of SFs are discussed in Section 4, and the procedure of SF alignment is given in Section 5.

2. Calculation of Telescope Lenses

Transport telescopes described herein are made according to the Keplerian scheme, i.e., in the form of two positive confocal lenses with focal lengths f_1 and f_2. If the optical axis of both lenses is aligned with the beam axis, for an axially symmetric beam it is only the spherical aberration that makes a significant contribution to the wavefront distortion of a beam passed through the telescopes. When such telescopes are used in a multistage laser, it is difficult to avoid parasitic lasing due to residual reflections of light from antireflective coatings of the lenses. Therefore, the lenses have to be tilted off normal by a certain angle. This results in two additional aberrations—astigmatism and coma. Astigmatism occurring when the beam passes through the first tilted lens can be easily compensated by tilting off normal the second lens in the orthogonal plane. But coma and spherical aberration remain. The necessity to minimize them determines the choice of the shape and focal lengths of the lenses.

A. Choosing the Lens Shape

The lens shape or the curvature of lens surfaces should be chosen so as to minimize aberrations. In transport telescopes, aberrations manifest themselves by spreading of the focal point (Fig. 1). With an ideal lens, all rays passing in parallel at any distance h from the axis will converge in a single point (ray 1). For an aberration lens (ray 3) the size Δy of the region occupied by the aberration spot depends on h. For coma and for a spherical aberration [16]

$$\Delta y_c = -\frac{3}{2}\frac{h^2}{f}\tan(\alpha)W^{\infty}, \tag{1}$$

$$\Delta y_s = \frac{h^3}{f^2}P^{\infty}, \tag{2}$$

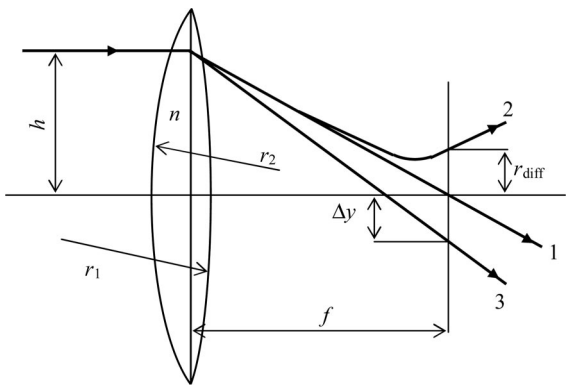

Fig. 1. Ray traces in a thin lens. Ray 1, no aberration, no diffraction; ray 2, diffraction, no aberration; ray 3, aberration, no diffraction.

where α is the angle of beam incidence on the lens, and the Seidel sums W^{∞} and P^{∞} for a thin lens are calculated by

$$P^{\infty} = \frac{n}{2(n-1)^2}\left[\frac{n+2}{n^2(1-C)^2} - \frac{2n+1}{n(1-C)} + n\right], \tag{3}$$

$$W^{\infty} = -\frac{2}{n-1}\left[n - \frac{n+1}{n(1-C)}\right]. \tag{4}$$

Here n is the refractive index of the lens material, r_1 and r_2 are the radii of spherical surfaces of the lens, and C is the ratio describing the lens shape:

$$C = r_1/r_2. \tag{5}$$

Formula (3) shows that the spherical aberration, i.e., parameter P^{∞} has a minimal value P_s at $C = C_s$:

$$P_s = P^{\infty}(C_s) = \frac{n(4n-1)}{8(n+2)(n-1)^2},$$
$$C_s = \frac{n(2n-1)-4}{n(2n+1)}. \tag{6}$$

However, in this case coma remains significant because $W_s = W^{\infty}(C_s) = (-1)/(n+2)$. On the other hand, it can be easily shown from Eq. (4) that for

$$C_c = 1 - \frac{1}{n} - \frac{1}{n^2} \tag{7}$$

coma becomes zero; i.e., $W_c = W^{\infty}(C_c) = 0$. In that case the value of spherical aberration assumes the form

$$P_c = P^{\infty}(C_c) = \frac{n^2}{2(n-1)^2}\left[\frac{n(n+2)}{(n+1)^2} - \frac{2n+1}{n+1} + 1\right]. \tag{8}$$

For $n < 2$ the value of P_c differs from its minimal value P_s of Eq. (6) by less than 1%. At $n = 1.5$ the minimal value of spherical aberration $P_s = 1.071$ will be for $C_s = -1/6$, and if we put coma to zero ($C_s = -1/9$), then $P_c = 1.08$. Thus, to have minimum aberrations in the telescope, one should choose a lens shape according to condition (7) so as to zero the coma rather than minimize the spherical aberration according to condition (6).

Let us compare the contributions of coma and spherical aberration to phase distortion and beam divergence. The coma contribution depends on the angle of beam incidence on the lens α and may be neglected at small α. On the other hand, at large α the coma contribution becomes more important. Let us, for example, consider a onefold telescope with a beam diameter of 10 cm ($h = 5$ cm) and a lens focal length of 350 cm. According to Eqs. (1) and (2) the beam displacement for coma Δy_c equals the beam displacement for spherical aberration Δy_s at $\alpha = 2°$. This means that one may completely neglect coma at

$\alpha \ll 2°$. From the viewpoint of the beam divergence (or M^2 parameter) for the above-mentioned telescope the coma contribution to the beam divergence may be neglected at $\alpha < 2°$. At $\alpha > 4°$ coma increases divergence and the M^2 parameter substantially and hence coma compensation is important. For example, at $\alpha = 10°$ use of the coma-compensated lens described in Eq. (7) instead of the spherical aberration compensated lens described in Eq. (6) reduces the M^2 parameter from 1.5 to 1.2 for the 8.5 cm diameter Gaussian beam.

In any case the divergence of a beam passed through any optical system consisting of the coma-compensated lens described in Eq. (7) is less than the divergence of the beam passed through the same optical system consisting of the spherical-aberration-compensated lens described in Eq. (6). Taking into account that the coma compensation does not require any special efforts (just to use the lens with the proper surface curvature radii), we may conclude that the coma compensation is justifiable in any case. It is also valuable to note that coma (on the contrary to spherical aberration) induces non-axially-symmetric phase distortions. Hence, spherical aberration suppression by an adaptive mirror is much easier than coma suppression.

The finite thickness d of lenses used in telescopes corrects to a certain degree values of parameters responsible for the spherical aberration described in Eq. (3) and the coma described in Eq. (4). The value of spherical aberration Δy_{sd} is less governed by the lens thickness. Direct calculations of Δy_{sd} by ray tracing [16] show that even for very thick lenses with $d \equiv 0.4f$ the value of Δy_{sd} is different by only 10% from an analogous value calculated by formula (2). As shown above, for a thin lens with $n = 1.5$ at $C = -1/9$ the coma is zero. For a thick lens it is difficult to totally zero the coma. However, as ray tracing shows, for a not very thick lens with $d < 0.1f$ the coma is always lower than the spherical aberration: $\Delta y_{cd} \ll \Delta y_{sd}$. We assume that the angle of lens tilt α is no more than 15°. Moreover, this inequality is valid not only for $C = -1/9$ but also for reasonable accuracies of lens fabrication $-0.12 < C < -0.1$.

Thus, although coma-induced distortions, in contrast to those caused by spherical aberrations, have azimuth variations of beam wavefront, the coma can always be neglected, provided the lens shape is optimal according to expression (7).

B. Choosing the Lens Focal Length

The above expressions allow us to determine a lens shape that would ensure minimal aberrations. However, the absolute value of these aberrations depends on focal lengths of the telescope lenses, and, besides, the spherical aberration is inversely proportional to the second power of f [see Eq. (2)]. As a result, there arises a problem of the minimal length $f_1 + f_2$ of the telescope providing high quality of radiation. Such a telescope should not considerably distort the wavefront; i.e., it should not significantly increase the divergence of laser radiation.

Minimal beam divergence is determined by the diffraction limit θ_d, which depends on the intensity distribution. Spherical aberrations increase the beam divergence. For a super-Gaussian beam with radius a, which is a convenient idealized case of bell-shaped beams, the complex field amplitude at the telescope output will be written as

$$E(r) = E_0 \exp\left(-\frac{r^{2m}}{2a^{2m}}\right)\exp\left(-iV\frac{r^4}{a^4}\right), \tag{9}$$

where V is expressed through the Seidel sums of telescope lenses P_{c1} and P_{c2} and telescope magnification $N = f_2/f_1$:

$$V = \frac{ka^4}{2}\frac{P_{c1} + P_{c2}N}{Nf_2^3}. \tag{10}$$

Here $k = 2\pi/\lambda$ is the wavevector. As the criterion of the minimal length of the telescope we may select a $\sqrt{2}$ times increase of the beam divergence θ due to the spherical aberration compared to the diffraction divergence θ_d,

$$\theta = \sqrt{2}\theta_d, \tag{11}$$

or a physically equivalent condition,

$$M^2 = \sqrt{2}M_d^2, \tag{12}$$

where M^2 is the beam quality criterion [17]. For a Gaussian beam, $\theta_d = 1/(ka)$ and $M_d = 1$. To calculate θ and M^2 for a beam with an arbitrary intensity profile and aberrational phase, one may use expressions for θ derived with the method of moments [18] or for the M^2 parameter [17,19]. As a result, for the laser field described in Eq. (9) we obtained

$$\theta^2 = {\theta_d}^2 + \frac{16V^2}{(ka)^2}\frac{\Gamma(4/m)}{\Gamma(1/m)}, \qquad {\vartheta_d}^2 = \frac{1}{(ka)^2}\frac{m^2}{\Gamma(1/m)}, \tag{13}$$

$$M^4 = {M_d}^4 + \frac{16V^2}{\Gamma(1/m)^2}[\Gamma(2/m)\Gamma(4/m) - \Gamma(3/m)^2],$$

$${M_d}^4 = \frac{m^2\Gamma(2/m)}{\Gamma^2(1/m)}, \tag{14}$$

where $\Gamma(x)$ is the Euler gamma function. The quadratic component of the divergence θ can be compensated for by means of a lens with a focal length of $F_{cor} = -(ka^2/4V)\,[\Gamma(2/m)/\Gamma(3/m)]$ [19] or by varying the distance between the telescope lenses by a distance of f_2^2/F_{cor}. In this case the beam divergence is given by

$$\theta^2 = \theta_d{}^2 + \frac{16V^2}{(ka)^2\Gamma(1/m)\Gamma(2/m)} \times [\Gamma(4/m)\Gamma(2/m) - \Gamma(3/m)^2]. \quad (15)$$

Equations (14) and (15) show that conditions (11) and (12) are equivalent to the equality of the focal radii of a nonaberrated beam with diffraction and a spherically aberrated beam without diffraction: $\Delta y = r_{\text{diff}}$ in Fig. 1. Substituting Eq. (15) into Eq. (11) or Eq. (14) into Eq. (12) and taking into account Eq. (10) yields an expression for the minimal focal length of a longer-focus lens of the telescope:

$$f_{\min} = \left(\frac{4\pi a^4}{\lambda m}\sqrt{\Gamma(4/m) - \frac{\Gamma(3/m)^2}{\Gamma(2/m)}}(P_{c1}/N + P_{c2})\right)^{1/3}. \quad (16)$$

In case of a onefold magnification telescope ($f_1 = f_2 = f, N = 1$) with an aperture radius of $R = 5$ cm for a Gaussian beam ($m = 1$) with $a = R/2.3$ (at the edge of the aperture R the intensity will be 10% of the axis intensity) the minimal length will be $2f = 400$ cm. For a flat-top beam ($m \to \infty$) with the same parameters, $2f = 562$ cm.

In many applications, of most interest is the far-field distribution or spatial spectrum. Figure 2 shows the radial electric-field distribution in the focal plane of an ideal lens for a beam with a flat phase profile and with aberrations introduced by the onefold magnification telescope with the optimal lens shape ($n = 1.5, C = -1/9$) both for the case when condition (16) is satisfied and when the focal length of the lens is twice as small as in condition (16).

It can be seen from Fig. 2 that even for a flat-top beam when condition (16) is fulfilled the field is localized close to the axis at distances comparable to the distances that are determined by diffraction. At the same time, when the telescope length becomes shorter, the focal spot is much blurred. Note that the Strehl ratio falls from $S = 1$ for an unaberrated beam to $S = 0.76$ after the telescope with $f = 274$ cm and even to $S = 0.098$ after the telescope with $f = 137$ cm. A detailed study of the dependences of different beam quality criteria on spherical aberration is given in [20].

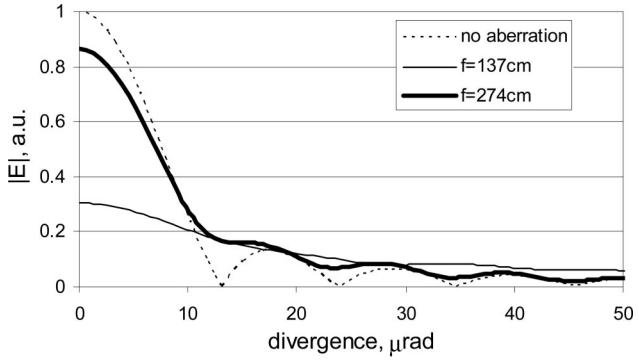

Fig. 2. Field amplitude module in the focal plane of an ideal lens for a flat-top beam with a radius of 49 mm ($\lambda = 1.05$ μm) without aberrations and with spherical aberrations induced by a onefold magnification telescope with optimal-shape lenses as described in Eq. (7) with focal lengths from Eq. (16) of $f = 274$ cm and $f = 137$ cm.

The criterion of beam quality described in Eq. (16) is weaker compared to the widely used Rayleigh and Marechal criteria [16] of image quality. Wavefront aberration at the beam edge must be less than $\lambda/4$ (Rayleigh) and $\lambda/14$ (Marechal). For the example shown in Fig. 2, the wavefront aberrations at the beam edge are 15λ and 2λ for a lens with a focal length of $f = 137$ cm and $f = 274$ cm, respectively.

3. Calculation of the Pinhole Diameter

A pinhole located in the focal plane of the telescope provides spatial filtering of the beam: it removes high-frequency components from the spatial spectrum. This is required to prevent parasitic lasing, to decrease amplified spontaneous emission (ASE), and to suppress small-scale self-focusing.

Parasitic lasing in a multistage laser amplifier is caused by residual reflections from different elements by small angles relative to the beam propagation direction. Common ways to suppress parasitic lasing include antireflection coatings on all elements of the system, tilting elements off and use of various nonreciprocal elements (Faraday isolators or Pockels cell gates). It is always preferred to have as small a number of isolators and gates as possible. When the quality of optical elements was high and spatial filters with a narrow angle of view were used, we managed to achieve a small signal gain coefficient of $G_0 = 10^6$–10^7 between two gates [14].

ASE noise is the fundamental noise that is always present in laser amplifiers. Its power, at a given G_0, can be decreased only by reducing the lifetime of high G_0 (by means of Pockels cell gates) or by narrowing the angle of view of the laser (by means of SFs).

An efficient way to suppress small-scale self-focusing is also to narrow the angle of view of the SF. Below we shall estimate the maximum angle of view or, which is the same, the maximum size of the SF pinhole for small-scale self-focusing suppression. Then we shall calculate the energy of the ASE noise in the laser with such an angle of view of the SF.

A. Suppression of Small-Scale Self-Focusing

When a high-power beam propagates in a transparent dielectric with cubic nonlinearity coefficient γ, the value of the refractive index depends on light intensity I:

$$n_{\text{NL}} = n_0 + \gamma_I, \quad (17)$$

where n_0 is the value of the refractive index at small intensities. If $\gamma > 0$, self-focusing of the beam may occur. For short laser pulses ($\tau < 10$ ns) the main mechanism that leads to dependence (17) is the Kerr effect. Relaxation times for the orientational Kerr effect (rotation of the molecule as a whole) is typically

of the order of 10^{-10}–10^{12} s for gaseous and liquid dielectrics, whereas for the electronic Kerr effect (direct distortion of the electron cloud) the relaxation times are much shorter—10^{-15} s. The typical value of γ for the electronic self-focusing is

$$\gamma = (3 - 5) \times 10^{-7}\ \mathrm{cm^2\ GW^{-1}}. \tag{18}$$

If intense radiation propagates as a bell-shaped beam, the peripheral rays whose intensity is lower than that of the central rays deviate from the beam axis because n_{NL} is lower for them than for the beam on the axis. This is self-focusing of the beam as a whole. If a flat-top beam with radius a propagates at a distance much shorter than the Rayleigh length $z_R = ka^2$, there is no self-focusing of the beam as a whole because n_{NL} is uniform over the entire beam cross section. However, small intensity spikes in the beam start growing, splitting the beam under certain conditions into separated threads. This leads to a sharp rise of the beam divergence and a breakdown in optical elements. This effect is called small-scale self-focusing.

The small-scale self-focusing theory shows [21] that there is an angular scale of inhomogeneities that maximally grow in the light wave of the intensity I (the theory assumes no amplification in the nonlinear medium):

$$\Theta_{\max} = \left(\frac{2\gamma}{n_0} I\right)^{1/2}. \tag{19}$$

A measure for the small-scale self-focusing, as well as for the beam self-focusing as a whole, is the B-integral. If a beam passes through a nonlinear layer with length L the value of the B-integral will be

$$B = k\gamma \int_0^L I(z)\mathrm{d}z. \tag{20}$$

In the case of whole-beam self-focusing, this will lead to a nonlinear lens with the characteristic focal length of

$$F_{\mathrm{NL}} = \frac{z_R}{2B}. \tag{21}$$

In the case of small-scale self-focusing, the intensity of speckles with the optimal angular scale described in Eq. (19) at the entrance to the nonlinear layer I_{in} will grow at the exit up to

$$I_{\mathrm{out}} = I_{\mathrm{in}} \exp(2B). \tag{22}$$

There are always intensity inhomogeneities in the beam, so during beam propagation through a number of amplifiers and other optical elements of a high-power laser, small-scale self-focusing will always lead to beam degradation and damage of laser elements. It is known with a high degree of probability [4,5] that, if in successively arranged optical elements the total value of the B-integral is larger than 2–3, then a threadlike structure is formed in the beam, causing multiple breakdowns in the optical elements.

A typical picture of the far-field region of a smooth bell-shaped beam profile with a characteristic radius a is a bright spot corresponding to angle $1/(ka)$. The spot is encircled by concentrically arranged diffraction rings with descending intensities. If a small-scale noise is present in the beam, in the far-field of such a beam there will be a ring with a radius of the angular component described in Eq. (19). If the inequality is satisfied,

$$\theta_{\max} = \left(\frac{2\gamma I}{n_0}\right)^{1/2} \gg \frac{1}{ka}, \tag{23}$$

a pinhole with a diameter D that obeys the condition

$$\theta_{\max} > \left(\frac{D}{2f}\right) \gg \frac{1}{ka} \tag{24}$$

and is situated in the lens focal plane of the spatial filter greatly reduces the maximally amplifying noise components described in Eq. (19). This is an underlying feature in the small-scale self-focusing suppression methods.

If the right-hand side of inequality (24) is disobeyed, i.e., high-frequency components of the beam itself are cut off, then after the SF the beam shape will be distorted. If the left-hand side of inequality (24) is disobeyed, the small-scale self-focusing will be only weakly suppressed.

We shall estimate a typical value of $\Theta_{\max}$ for phosphate laser glass, the main contributor to the total value of the B-integral. For $I = (1\text{–}10)\ \mathrm{GW/cm^2}$ (damage threshold for transparent dielectrics is about $20\ \mathrm{GW/cm^2}$ at 1 ns pulse duration) expressions (18) and (19) yield $\theta_{\max} = (0.64 - 2) \times 10^{-3}$. For $\lambda = 1\ \mu\mathrm{m}$ this corresponds to the characteristic size of small-scale perturbations $a_{\max} = (0.26 - 0.08)$ mm.

These estimations show that for amplifiers based on phosphate glass with a diameter of $2R \geq 10$ cm, the SF that efficiently suppresses small-scale self-focusing and only slightly distorts the transverse beam distribution can be quite easily implemented. For $R < 5$ cm the efficiently suppressing SF will always, in a varying degree, distort the transverse distribution of the beam. To minimize these distortions, it is necessary to make them symmetric with respect to the beam axis. Therefore, precise matching of the SF pinhole to the beam axis is required (see Section 5 for more details).

B. Suppression of Amplified Spontaneous Emission

ASE noise is inevitable in laser amplifiers and its power considerably depends on the angle of view. We shall estimate the ASE noise in an amplifier with an angle of view of $\Delta\Omega$. We assume that the gain has a

Table 1. Parameters of Lenses Used in Spatial Filters of the 300 J 1 ns Laser

#	Input/Output Beam Diameter (mm)	f_1 (mm) r_1 (mm)	f_1 (mm) r_2 (mm)	f_2 (mm) r_1 (mm)	f_2 (mm) r_2 (mm)	Lens Diameter/ Thickness (mm)	P_1^{∞}	P_2^{∞}	W_1^{∞}	W_2^{∞}
1	30/60	1076		2326		120/12	1.053	1.053	0.228	0.242
		1076	2326	1355	8954					
2	60/85	1628		2326		160/16	1.053	1.053	0.175	0.242
		938	6792	1355	8954					
3	85/100	2291		2639		160/16	1.053	1.053	0.328	0.256
		1355	8017	1542	10000					
4	100/130	3555		4603		180/18	1.057	1.063	−0.07	0.026
		2012	17036	2563	25696	(160/18)				

Gaussian time profile with width Δt, Gaussian spectra with bandwidth $\Delta\omega$, and maximum value G_0. For simplicity, we consider that the amplifier is a long cylindrical rod placed in an immersion liquid. We shall also neglect the radial dependence of the gain coefficient. Under these assumptions, the noise density at the output of the amplifier can be estimated by formula [22]:

$$w_{\mathrm{ASE}} = \frac{\hbar c n_0^2 G_0 \Delta\omega \Delta\Omega \Delta t}{\ln 2 \lambda^3 \ln G_0}. \tag{25}$$

In a multicascade phosphate glass amplifier with $n_0 = 1.6$, $G_0 = 2.3 \times 10^6$ with a solid angle of view not limited by a SF (no spatial filtration), $\Delta\Omega = 2.9 \times 10^{-3}$ sr, the noise energy density is $W_{\mathrm{ASE}} = 0.32\ \mathrm{J/cm^2}$. This value is lower than the saturation fluence of neodymium phosphate glass ($3.5\ \mathrm{J/cm^2}$) and cannot significantly reduce the gain coefficient. Nevertheless, at an aperture radius of $R = 5$ cm the total noise energy at the output of the amplifier will be 25 J. With increasing G_0 up to 10^7 the noise energy density will grow up to $W_{\mathrm{ASE}} = 1.26\ \mathrm{J/cm^2}$, a value comparable with the saturation fluence.

In the case of a SF with an angle of view satisfying condition (24), for the above amplifier $\Delta\Omega = 1.26 \times 10^{-7}$ sr, the noise energy density even at $G_0 = 10^7$ will be negligibly small, $W_{\mathrm{ASE}} = 5.5 \times 10^{-5}\ \mathrm{J/cm^2}$. Thus the use of the pinhole in the SF that satisfies condition (24) will decrease the ASE noise energy density down to negligibly small values compared to the saturation fluence density of the lasing transition.

4. Spatial Filter Design

Various SF designs are possible, though we believe that the most reliable and easy-to-operate one is the design used in a Nd:glass laser [14] whose radiation served for pumping of a powerful optical parametric amplifier [11,12]. Below we shall describe this SF design in more detail.

In the Nd:glass laser described in [14] three SFs were used. All of them were designed for minimum spherical aberration as described in Eq. (6). In this amplifier, the diffraction-limited beam quality was not important, so condition (6) was quite sufficient. When the setup was modified for pulse energies of 300 J [23], an additional SF was included in the laser output to broaden the output beam diameter up to 130 mm. Its lenses obey condition (7). Lens parameters of all four SFs are presented in Table 1.

Most sensitive to wavefront distortions of the beam is SF 3, which matches amplifier apertures with diameters of 85 and 100 mm. For compactness, lenses with focal lengths of $f_1 = 2291$ mm and $f_2 = 2639$ mm, respectively, were used in the telescope. These focal lengths fulfill the most stringent criterion—criterion (16) for a flat-top beam ($m = \infty$). The focal lengths of other telescopes were even longer than that for Eq. (16), so they did not noticeably distort the wavefront of the beam.

The SF is a thick-wall metal cell attached to a vacuum pipeline by a flexible corrugated metal hose. Pressure in the pipeline is kept at 10^{-3} Torr.

Telescope lenses made of K8 glass ($n = 1.506$) serve as the cell windows. The lens thickness is 10 times smaller than their diameter. The lens diameter is 1.5–2 times greater than the beam diameter and therefore mounting them by the edge using silastic does not introduce noticeable depolarization into the laser beam. The lenses are attached to the cell via flanges on flexible metal bellows so that the lenses can be tilted and the distance between them can be varied. Both lens surfaces are covered with antireflection coating.

A pinhole made of 0.2 mm thick tantalum foil is placed in the focal plane of the lenses. Relatively heavy tantalum ions due to their great inertia cannot close the pinhole during the 1 ns pulse [24]. The pinhole image was observed by CCD camera through a special vacuum window in the metal cell. The pinhole is mounted on a three-coordinate precision stage placed inside the cell. The stepper motors are remotely controlled with an analog device or a computer. The device can position the pinhole with an accuracy of ± 5 μm with a step of 2 μm. This accuracy is quite sufficient for SF alignment. The alignment procedure will be discussed in the following section.

5. Alignment of Spatial Filters

The alignment procedure included five successive steps: centering the lenses, preliminary transverse alignment of the pinhole, longitudinal alignment of

the pinhole, precise transverse alignment of the pinhole, and longitudinal alignment of lenses.

The centering of lenses was done in the following manner. First we visually aligned the beam axes with the center of the input lens. Then the pinhole was completely moved out of the telescope axis. Then, we matched the beam position at the output with the center of the output lens by changing the direction of the incident beam by means of a mirror. After that, the lens position was fixed, and alignment of the pinhole was made.

The typical value of the pinhole diameter in the telescopes is 1 mm, and the typical value of the beam waist diameter is about 100 μm. Therefore, rough alignment with accuracy up to about 100 μm was made by visually matching the pinhole center with the beam center (the SF metal cell has a window in its central part).

We adjusted the pinhole along the beam axis using an additional measurement long-focus lens placed after the telescope's output lens. The image of the focal plane of the telescope is exactly in the focal plane of this long-focus lens. To illuminate the pinhole, we placed a thin aberrator before the input lens of the telescope. By sharpness of the picture of the pinhole edge we managed to adjust the pinhole with an accuracy of up to ±100 μm. This size is much smaller than the waist length, so this accuracy is quite acceptable.

To precisely match the center of the pinhole with the beam axis, we placed before the input telescope lens an additional pinhole with a diameter 10–20 times smaller than that of the input beam. The ring structure in the far field enables high-precision matching of the pinhole to the laser beam (Fig. 3) [25]. The repeatability of this pinhole alignment is lying in the interval of ±5 μm. This precise alignment procedure was automated using a computer code written by the following algorithm. The center of the diffraction pattern was found as the center of symmetry of the pinhole illumination distribution. By the center of symmetry we understood a point, relative to which transformations of the intensity pattern distort the initial distribution to a lesser degree. We found the minimum of the self-similarity:

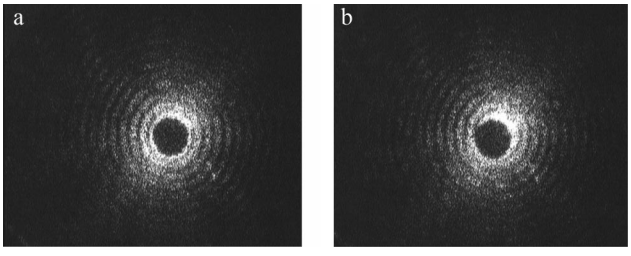

Fig. 3. Alignment picture viewed through a vacuum cell window in a SF when an additional pinhole with a diameter 10 times smaller than the beam diameter is placed before the input lens: (a) fine alignment of the pinhole, (b) detuning from fine alignment by 140 μm horizontally and 115 μm vertically. The pinhole diameter is 1 mm.

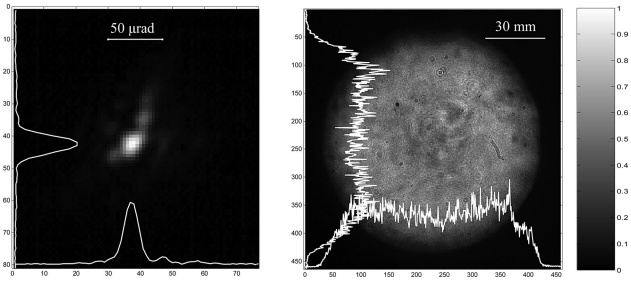

Fig. 4. Near and far field of the output beam of a 300 J 1 ns laser.

$$F = 1 - \frac{\sum_{i=1}^{M} (I_0,\ I_i)}{(I_0,\ I_0)M}.$$

Here I_0 is the intensity matrix fixed by the CCD camera, I_i is the intensity matrix after one of the symmetry transforms (central inversion, 180° rotation, 90° rotation, and so on), and M is the number of transforms. Typically we used $M = 7$. Thus we determined the center of the symmetry of the pattern. Then the pinhole moves to the center of the diffraction pattern. The total automated procedure takes about 1 min.

Finally, the distance between lenses was chosen so that the collimated beam incident on the telescope had minimal divergence at the output. To achieve this, we minimized the size of the intensity distribution in the focal plane of an aberration-free long-focus objective.

6. Conclusion

Due to the four spatial filters calculated, manufactured, and adjusted as shown above, we could arrange a compact six-stage Nd:glass amplifier with an energy of 300 J and a pulse duration of 1 ns. Output beam divergence was not more than 3–4 diffraction limits (see Fig. 4) at a filling factor of 0.8. Comparison of the far-field distribution with theoretical calculation based on aberration analysis described in Section 2 shows that spherical aberration makes the largest contribution to the beam divergence. That is a result of the coma-compensated lens described in Eq. (7) used in the final spatial filter and small incident angles ($\alpha < 1°$) used in all the other filters. To avoid parasitic oscillation at such small angles α, we used two Faraday isolators in the laser amplifier chain.

The above-described procedure of spatial filter alignment is simple and convenient; minor beam drifts in all four spatial filters can be adjusted for 15–30 min. Due to the high stability of the telescope design, the laser can operate without alignments during the whole working day.

References

1. G. H. Miller, E. I. Moses, and C. R. Wuest, "The National Ignition Facility," Opt. Eng. **43,** 2841–2853 (2004).
2. S. Nakai, T. Kanabe, T. Kawashima, M. Yamanaka, Y. Izawa, M. Nakatuka, R. Kandasamy, H. Kan, T. Hiruma, and M.

Niino, "Development of high-average-power DPSSL with high beam quality," Proc. SPIE **4065,** 29–39 (2000).
3. C. M. Bibeau, R. J. Beach, A. J. Bayramian, J.-C. Chanteloup, C. A. Ebbers, M. A. Emanuel, C. D. Orth, J. E. Rothenberg, K. I. Schaffers, J. A. Skidmore, S. B. Sutton, L. E. Zapata, S. A. Payne, and H. T. Powell, "Mercury and beyond: diode-pumped solid state lasers for inertial fusion energy," Proc. SPIE **3886,** 57–68 (2000).
4. D. R. Speck, "The Shiva Laser-Fusion Facility," IEEE J. Quantum Electron. **QE-17,** 1599–1619 (1981).
5. J. Bunkenberg, J. Boles, D. C. Brown, J. Eastman, J. Hoose, R. Hopkins, L. Iwan, S. D. Jacobs, J. H. Kelly, S. Kumpan, S. Letzring, D. Lonobile, L. D. Lund, G. Mourou, S. Refermat, W. Seka, J. M. Soures, and K. Walse, "The omega high-power phosphate-glass system: design and performance," IEEE J. Quantum Electron. **QE-17,** 1620–1628 (1981).
6. D. M. Pennington, M. D. Perry, B. C. Stuart, R. D. Boyd, J. A. Britten, C. G. Brown, S. M. Herman, J. L. Miller, H. T. Nguyen, B. W. Shore, G. L. Tietbohl, and V. Yanovsky, "Petawatt laser system," Proc. SPIE **3047,** 490–500 (1997).
7. Y. Kitagawa, H. Fujita, R. Kodama, H. Yoshida, S. Matsuo, T. Jitsuno, T. Kawasaki, H. Kitamura, T. Kanabe, S. Sakabe, K. Shigemori, N. Miyanaga, and Y. Izawa, "Prepulse-free petawatt laser for a fast ignitor," IEEE J. Quantum Electron. **40,** 281–293 (2004).
8. C. N. Danson, P. A. Brummitt, R. J. Clarke, J. L. Collier, G. Fell, A. J. Frackiewicz, S. Hancock, S. Hawkes, C. Hernandez-Gomez, P Holligan, M. H. R. Hutchinson, A. Kidd, W. J. Lester, I. O. Musgrave, D. Neely, D. R. Neville, P. A. Norreys, D. A. Pepler, C. J. Reason, W. Shaikh, T. B. Winstone, R. W. W. Wyatt, and B. E. Wyborn, "Vulcan petawatt—an ultra-high-intensity interaction facility," Nucl. Fusion **44,** S239–S249 (2004).
9. M. Aoyama, K. Yamakawa, Y. Akahane, J. Ma, N. Inoue, H. Ueda, and H. Kiriyama, "0.85-PW, 33-fs Ti:sapphire laser," Opt. Lett. **28,** 1594–1596 (2003).
10. I. N. Ross, P. Matousek, M. Towrie, A. J. Langley, and J. L. Collier, "The prospects for ultrashort pulse duration and ultrahigh intensity using optical parametric chirped pulse amplifiers," Opt. Commun. **144,** 125–133 (1997).
11. V. V. Lozhkarev, G. I. Freidman, V. N. Ginzburg, E. V. Katin, E. A. Khazanov, A. V. Kirsanov, G. A. Luchinin, A. N. Mal'shakov, M. A. Martyanov, O. V. Palashov, A. K. Poteomkin, A. M. Sergeev, A. A. Shaykin, I. V. Yakovlev, S. G. Garanin, S. A. Sukharev, N. N. Rukavishnikov, A. V. Charukhchev, R. R. Gerke, and V. E. Yashin, "200 TW 45 fs laser based on optical parametric chirped pulse amplification," Opt. Express **14,** 446–454 (2006).
12. V. V. Lozhkarev, S. G. Garanin, R. R. Gerke, V. N. Ginzburg, E. V. Katin, A. V. Kirsanov, G. A. Luchinin, A. N. Mal'shakov, M. A. Martyanov, O. V. Palashov, A. K. Poteomkin, N. N. Rukavishnikov, A. M. Sergeev, S. A. Sukharev, E. A. Khazanov, G. I. Freidman, A. V. Charukhchev, A. A. Shaykin, and I. V. Yakovlev, "100-TW femtosecond laser based on parametric amplification," JETP Lett. **82,** 178–180 (2005).
13. V. I. Kryzhanovskiĭ, B. M. Sedov, V. A. Serebryakov, A. D. Tsvetkov, and V. E. Yashin, "Formation of the spatial structure of radiation in solid-state laser systems by apodizing and hard apertures," Sov. J. Quantum Electron. **13,** 194–198 (1983).
14. A. K. Poteomkin, E. V. Katin, A. V. Kirsanov, G. A. Luchinin, A. N. Mal'shakov, M. A. Martyanov, A. Z. Matveev, O. V. Palashov, E. A. Khazanov, and A. A. Shaykin, "Compact 100 J/100 GW Nd:phosphate laser for optical parametric chirped pulse amplifier pumping," Quantum Electron. **35,** 302–310 (2005).
15. N. B. Kuz'mina, N. N. Rozanov, and V. A. Smirnov, "On spatial filtration of apodized laser beams," Opt. Spectrosc. **51,** 509–514 (1981).
16. M. Born and E. Wolf, *Principles of Optics* (Pergamon, 1980).
17. A. E. Siegman, "New developments in laser resonators," Proc. SPIE **1224,** 2–14 (1990).
18. S. N. Vlasov, V. A. Petrishchev, and V. I. Talanov, "Averaged description of wave beams in linear and nonlinear media," Izv. VUZov Radiophysics **14,** 1353–1363 (1971).
19. A. K. Poteomkin and E. A. Khazanov, "Calculation of the M^2 factor of the laser beam by the method of moments," Quantum Electron. **35,** 1042–1044 (2005).
20. E. Perevezentsev, A. Poteomkin, and E. Khazanov, "Comparison of laser beam quality criteria," Proc. SPIE **6101,** 610119 (2006).
21. V. I. Bespalov and V. I. Talanov, "Filamentary structure of light beams in nonlinear liquids," JETP Lett. **3,** 307–310 (1966).
22. A. I. Makarov and A. K. Potemkin, "Maximum gain of a multistage laser amplifier," Quantum Electron. **15,** 692–694 (1985).
23. A. A. Shaykin, E. V. Katin, E. A. Khazanov, A. V. Kirsanov, G. A. Luchinin, A. N. Mal'shakov, M. A. Martyanov, and A. K. Poteomkin, "Tabletop 300 J 1 ns Nd:glass laser," in *International Conference on High Power Laser Beams: Nizhny Novgorod—Yaroslavl—Nizhny Novgorod* (Institute of Applied Physics, 2006), paper 98.
24. R. G. Bikmatov, C. D. Boley, I. N. Burdonski, V. M Chemyak, A. V. Fedorov, A. Y. Goltsov, V. N. Kondrashov, S. N. Koptyaev, N. G. Kovalsky, V. N. Kuznetsov, D. Milam, J. Murray, M. I. Pergament, V. M. Petryakov, R. V. Smirnov, V. I. Sokolov, and E. V. Zhuzhukalo, "Pinhole closure in spatial filters of large-scale ICF laser systems," Proc. SPIE **3492,** 510–523 (1998).
25. A. F. Aushev, V G. Borodin, I. A. Bubnov, B. I. Venzel, S. G. Garanin, A. V. Gorelov, I. N. Derkach, L. V. L'vov, T. P. Malinova, V. U. Matveev, U. V. Mihailov, N. V. Nikitin, S. L. Potapov, N. V. Cidorovskii, A. B. Smirnov, A. N. Starchenko, S. A. Suharev, A. V. Ugryumov, V. G. Filippov, A. V. Charuhchev, and V. N. Chernov, "Remote alignment system for four-channel Nd-glass-based laser facility LUCH," J. Opt. Technol. **70,** 56–64 (2003).